Crystallization of Polypropylene in the Presence of a Rigid and Flexible Additive

K. Prakashan, A. K. Gupta, S. N. Maiti

Centre for Polymer Science and Engineering, Indian Institute of Technology Delhi, New Delhi 110016, India

Received 23 August 2007; accepted 25 November 2007
DOI 10.1002/app.27751
Published online 23 January 2008 in Wiley InterScience (www.interscience.wiley.com).

ABSTRACT: The effect of a rigid additive (nano-SiO_2 filler) and a flexible additive [poly(dimethylsiloxane) elastomer] on the crystallization of polypropylene was studied under nonisothermal conditions with differential scanning calorimetry. Crystallization parameters were evaluated with standard equations, and the results were interpreted on the basis of the rate of nucleation, crystallization, and activation energy of crystallization. The observed effect of polydimethylsiloxane of increasing the crystallization rate and lowering the activation energy of crystallization was attributed to the effect of polydimethylsiloxane chain mobility at the interface, which facilitated the molecular mobility of polypropylene. Nano-SiO_2, on the other hand, acted as a nucleating agent, and the nucleation effect was dependent on the cooling rate. © 2008 Wiley Periodicals, Inc. J Appl Polym Sci 108: 1298–1306, 2008

Key words: crystallization; nanocomposites; poly(propylene) (PP)

INTRODUCTION

The crystallization of polypropylene (PP) in the presence of various fillers and additives has been exclusively studied, and interest still continues because of its importance in the processing behavior, crystalline morphology, and properties of the final product. Additives are incorporated into PP to improve the crystallization behavior and various properties. Effects of additives on the crystallization behavior and crystalline morphology are quite significant because of the fast crystallizing nature of PP. Thus, reinforcing fillers in PP composites and polymers used as second components in PP blends may act in two ways: (1) producing reinforcement or rubber toughening and (2) modifying the crystallization behavior and crystalline morphology.

Reinforcing fillers such as calcium carbonate,[1] talc,[2] mica,[3] montimorillonite,[4] carbon black,[5] carbon nanofiber,[6] carbon nanotubes,[7] glass fiber,[8] silicon dioxide (SiO_2),[9] and polyhedral silsesquioxane [10] affect the crystallization of PP. Polymeric inclusions such as poly(ethylene–propylene rubber),[11] polyisobutylene,[11] polystyrene,[12] styrene–butadiene elastomeric nanoparticles,[13] polycarbonate,[14] high-density polyethylene,[15] poly(phenylene sulfide),[16] hyperbranched polyurethane acrylate,[17] and maleic anhydride grafted PP[18] have also been reported to affect the crystallization of PP.

In this article, we report a study of two additives, a rigid filler (i.e., nano-SiO_2) and a flexible polymer [i.e., poly(dimethylsiloxane) (PDMS) elastomer], on the nonisothermal crystallization kinetics of PP. These two additives give rise to distinctly different natures of the interface, which may affect the crystallization behavior of PP. The crystallization process depends on the nucleation and ease of chain mobility of the crystallizing polymer. Among the two additives chosen in this study, one (i.e., nano-SiO_2 filler) is expected to affect nucleation, whereas the other (i.e., PDMS elastomer) may have some influence on molecular chain mobility in the interface regions.

EXPERIMENTAL

Materials

The PP used in this study was a homopolymer, Repol H200MK, produced by Reliance Industries, Ltd. (Mumbai, India; melt flow index = 20 at 230°C and 2.16 kg). The nano-SiO_2 was hydrophilic fumed silica nanoparticles supplied by Wacker Chemie AG (Munich, Germany) under the trade name Wacker HDK N 20. It had a surface area of 200 m^2/g. The particle sizes of the water suspension of nano-SiO_2 were determined with a Brookhaven (Brookhaven Instrument Corporation, Holtsville, NY) 90 Plus particle size analyzer working on the principle of dynamic light scattering. The particle sizes were in the range of 100–500 nm with mean and median diameters of 261 and 232 nm, respectively. The PDMS elastomer used was a noncommercial grade (Silpren V-SS), with no filler or additive, and was obtained from GE Bayer

Correspondence to: A. K. Gupta (akgncute@hotmail.com).

Journal of Applied Polymer Science, Vol. 108, 1298–1306 (2008)

Silicones (Bangalore, India). The molecular weight of PDMS was 250000, as determined by intrinsic viscosity measurements in toluene using the values of the constants k and a of Mark-Houwink equation for the same polymer-solvent system.[19]

Blending and injection molding

Blending was carried out in a JSW J75E IV-P twin-screw extruder made by Japan Steel Works Ltd. (Tokyo, Japan), with a length/diameter ratio of 36 and a diameter of 30 mm. The materials were predried in a vacuum oven at 70°C for 3 h before blending. Extrusion was performed at a screw speed of 250 rpm with the temperature profile of 140–150–190–205–205–205–215–215–225–230°C from the feed zone to the die zone. The extruded strands were quenched in a water bath and granulated. The granules were then dried in a vacuum oven at 70°C for 2 h and injection-molded with a Demag L&T PFY 40 injection-molding machine (L&T-Demag Plastics Machinary Pvt. Ltd., Chennai, India). The barrel temperature profile of the injection molding was 190–220–225–230°C, whereas the mold was at room temperature. The compositions and nomenclature of the various samples thus prepared are given in Table I. Letters E and S in the sample names indicate the elastomer (PDMS) and nano-SiO_2 contents, respectively, and the digits following them denote their proportions in parts by weight.

Differential scanning calorimetry (DSC)

The nonisothermal crystallization thermograms were recorded on a PerkinElmer (Waltham, MA) Pyris-7 differential scanning calorimeter with the temperature calibrated with indium. Sample pieces of 5–6 mg, cut from the injection-molded specimens, were used for DSC measurements. Samples were heated from room temperature to 200°C and held there for 2 min to eliminate the residual crystals and memory effects of thermal and shear history, and subsequently the melt was cooled to crystallize at four different cooling rates (5, 10, 20, and 30°C/min) under a nitrogen atmosphere to room temperature to record the DSC thermograms.

TABLE I
Description and Composition of the PP/PDMS Blends and PP/Nano-SiO_2 Composites

Sample	PP (parts by weight)	PDMS (parts by weight)	Nano-SiO_2 (parts by weight)
PP	100	0	0
PP/E5	100	5	0
PP/E10	100	10	0
PP/E20	100	20	0
PP/E30	100	30	0
PP/S2	98	0	2
PP/S4	96	0	4
PP/S6	94	0	6

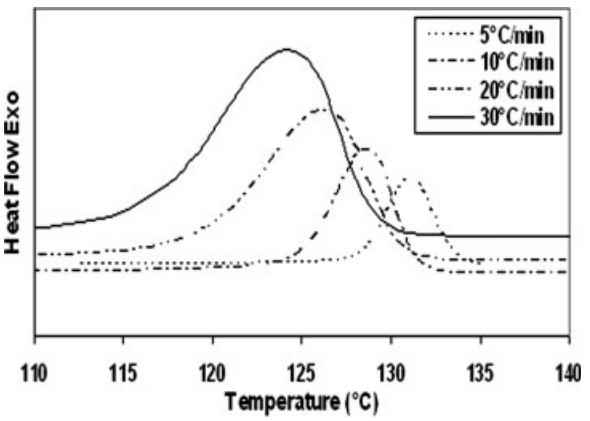

Figure 1 Crystallization exotherms of PP at various cooling rates.

RESULTS AND DISCUSSION

DSC results

Some representative DSC thermograms are presented in Figures 1–3 to show the effect of the variation of the cooling rate and additive content on the crystallization exotherm of PP. Figure 1 shows crystallization exotherms of PP recorded at different cooling rates. With the cooling rate increasing, the curve broadens and shifts to lower temperatures. This is consistent with the general belief that at higher cooling rates, the activation of nuclei formation occurs at lower temperatures, whereas at lower cooling rates, crystallization occurs at higher temperatures.[20] Figures 2 and 3 show the effects of the nano-SiO_2 filler content and PDMS elastomer content on the exotherm at a constant cooling rate of 5°C/min, respectively. The addition of nano-SiO_2 results in a shift of the exotherm toward a higher temperature than that of PP (Fig. 2), and this implies that the

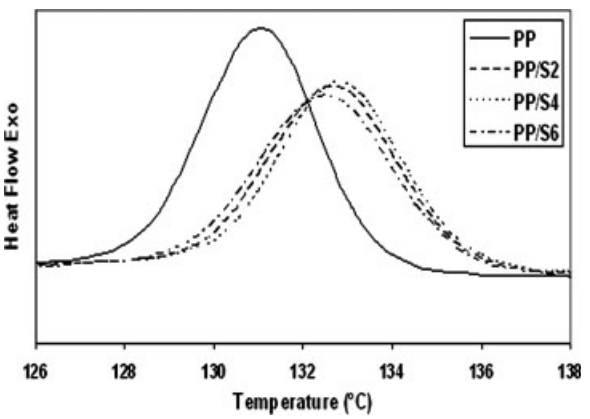

Figure 2 DSC crystallization exotherms for PP and PP/nano-SiO_2 composites at 5°C/min.

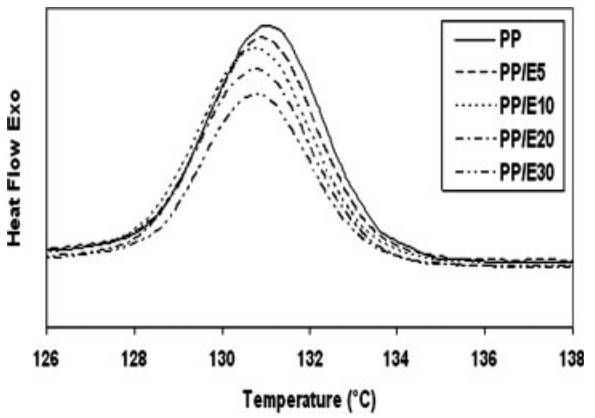

Figure 3 DSC crystallization exotherms for PP and PP/PDMS blends at 5°C/min.

addition of nano-SiO_2 activates nucleation at higher temperatures and causes crystallization to occur at higher temperatures. The variation of the crystallization temperature (i.e., peak temperature) with the filler content is quite small, showing very little variation in the effect of the nano-SiO_2 filler content beyond the initial addition of 2 wt %. On the other hand, the addition of PDMS to PP produces almost no shift or a very small decrease of the crystallization peak temperature with respect to that of PP (Fig. 3). The PDMS content variation affects the peak height (and peak area), and this may be attributed to the decreasing proportion of the crystallizing component (PP) of the blend with increasing PDMS content.

A characterization of the changes in the exotherm produced by the additives in terms of the following parameters provides interesting insight into the effect of these additives on the crystallization of PP. The characteristic parameters of the exotherm used here are the crystallization initiation temperature of the exotherm (T_i), the crystallization peak temperature (T_p), and enthalpy of crystallization (ΔH_c) calculated from the area of the exotherm.

Values of the exotherm parameters for the PP/nano-SiO_2 system are presented in Table II. T_i increases upon the initial 2 wt % addition of nano-SiO_2 filler, and thereafter the value remains unchanged upon further increase of the filler content up to 6 wt %. This type of leveling off of nucleation activity beyond a particular concentration of the nucleating agent has been reported for other nucleating agents also.[21] The increase in T_i is prominent only at the cooling rates of 5 and 10°C/min, but at the higher cooling rates of 20 and 30°C/min, there is no increase in T_i produced upon the addition of nano-SiO_2 filler. It may be possible that at a lower cooling rate, with which molecules get enough time for nucleation, nucleation on the already available surface of nano-SiO_2 particles is preferred in comparison with nucleation on the heterogeneous or homogeneous nuclei inherently present in PP, which generally have an induction time. However, at a higher cooling rate, the nuclei are initiated at a lower temperature in a very short time, so it is possible that nucleation proceeds instantaneously on the nano-SiO_2 surface as well as the homogeneous nuclei (other than those induced by nano-SiO_2) present in the system.

The T_p value increases upon the initial 2 wt % addition of the nano-SiO_2 filler, and thereafter the value remains unchanged with a further increase of the filler content up to 6 wt % at each cooling rate studied. The magnitude of this increase of the T_p value decreases gradually from 1.6 to 0.5°C as the cooling rate increases from 5 to 30°C/min. The occurence of a slightly higher T_p value at the cooling rates of 20 and 30°C/min, at which there is no change in the T_i value observed upon the addition of nano-SiO_2, is an indication of a faster crystallization rate for PP/nano-SiO_2 composites at these cooling rates. It may be possible that the combined activation of nucleation on the nano-SiO_2 surface and on the homogeneous nuclei present (other than those induced by nano-SiO_2) at a higher cooling rate can result in a large increase in the number of nucleation sites and thus in the increase of rate of crystallization. The results of a later section also support this reasoning.

ΔH_c decreases with the cooling rate increasing, and this indicates a lower degree of crystallinity in the sample crystallized at a faster cooling rate. The addition of nano-SiO_2 filler reduces the degree of crystallinity, as observed at each of the cooling rates studied. The decrease of ΔH_c occurs mainly in the first-step addition of the filler (i.e., at 2 wt %), and thereafter it becomes relatively small; this indicates the smaller effect of the variation of the nano-SiO_2 filler content on the degree of crystallinity of PP beyond the filler content of 2 wt %.

TABLE II
Crystallization Exotherm Parameters for PP and PP/Nano-SiO_2 Composites

R (°C/min)	Sample	T_i (°C)	T_p (°C)	ΔH_c (J/g)
5	PP	135.3	131.0	101.30
	PP/S2	137.4	132.6	94.99
	PP/S4	138.0	132.8	96.56
	PP/S6	137.4	132.5	90.67
10	PP	133.3	128.6	98.71
	PP/S2	135.3	129.9	96.22
	PP/S4	135.4	129.8	96.81
	PP/S6	135.0	129.7	94.50
20	PP	132.3	125.5	93.77
	PP/S2	132.4	126.2	91.80
	PP/S4	132.3	126.2	92.26
	PP/S6	132.2	126.2	90.88
30	PP	132.0	123.8	93.11
	PP/S2	131.9	124.3	90.50
	PP/S4	132.0	124.4	89.68
	PP/S6	132.1	124.0	91.20

TABLE III
Crystallization Exotherm Parameters for PP and PP/PDMS Blends

R (°C/min)	Sample	T_i (°C)	T_p (°C)	ΔH_c (J/g)
5	PP	135.3	131.0	101.30
	PP/E5	134.7	130.9	92.90
	PP/E10	134.6	130.8	91.74
	PP/E20	134.5	130.7	87.27
	PP/E30	134.7	130.9	74.45
10	PP	133.3	128.6	98.71
	PP/E5	132.7	128.0	93.93
	PP/E10	132.6	128.2	92.53
	PP/E20	132.7	128.5	77.27
	PP/E30	132.8	128.4	82.08
20	PP	132.3	125.5	93.77
	PP/E5	130.0	125.2	89.17
	PP/E10	130.3	125.2	87.05
	PP/E20	130.2	125.2	76.53
	PP/E30	130.2	124.8	72.05
30	PP	132.0	123.8	93.11
	PP/E5	129.4	123.4	89.23
	PP/E10	129.2	123.3	74.82
	PP/E20	129.1	123.1	76.32
	PP/E30	129.3	123.2	71.80

Values of the exotherm parameters for the PP/PDMS system are presented in Table III. T_i decreases with the addition of PDMS, and the magnitude of this decrease increases with the cooling rate increasing. However, there is no systematic variation of the decrease in the T_i value observed with the PDMS content. This indicates a delaying effect of nucleation produced by PDMS, which becomes more prominent at faster cooling rates and is very little affected by the variation of the PDMS content of the blend.

T_p decreases by less than 1°C upon the addition of PDMS, and the decrease is quite systematic as a function of the cooling rate. However, there is no systematic variation of the decrease in the T_p value with increasing elastomer content. It is to be noted that the magnitude of the decrease of T_p is less than that of the decrease in T_i for all the blend samples at all cooling rates, and this indicates faster crystallization in the presence of PDMS. Results in the later sections also confirm this observation.

The parameter ΔH_c, related to the degree of crystallinity of a sample, decreases upon the addition of PDMS at each of the cooling rates studied. This decrease of crystallinity continues with increasing elastomer content up to the highest value of elastomer content. In this respect, it differs from the case of the nano-SiO_2 filler, which produces a much smaller decrease of ΔH_c or the degree of crystallinity of PP. The unbalanced surface forces of nano-SiO_2 particles with the polymer interface may impede polymer chain mobility, and this might be the cause of the observed decrease of the degree of crystallinity of PP upon the addition of nano-SiO_2.

Crystallization kinetics

The crystallization kinetics are described by the following equation, in which the crystallinity fraction at any given time t, $[X(t)]$, is described as the ratio of the crystallinity developed up to time t (i.e., the area of the exotherm up to time t) to the total crystallinity developed from the onset to the end of the exotherm (i.e., the area of the total exotherm from the onset to the end):

$$X(t) = \frac{\int_{T_0}^{T} (dH_c/dT)dT}{\int_{T_0}^{T_\infty} (dH_c/dT)dT} \quad (1)$$

where T_0 and T_∞ represent the temperatures of the onset and end of the crystallization exotherm, respectively, and H_c is the enthalpy of crystallization. The development of $X(t)$ as a function of temperature for PP calculated from the observed exotherms at various cooling rates is shown in Figure 4 as a typical example. The curves of $X(t)$ versus temperature for the PP/PDMS and PP/nano-SiO_2 systems were qualitatively similar to that of PP shown in Figure 4, having a sigmoidal shape and showing a lag effect of the cooling rate on the crystallization process. The temperature axis in Figure 4 can be transformed to a timescale with the appropriate cooling rate. The curves of $X(t)$ versus time t thus obtained for PP at various cooling rates are presented in Figure 5. The $X(t)$–t curves for the studied PP/PDMS and PP/nano-SiO_2 systems were qualitatively similar to the curves shown in Figure 5.

On the basis of the Avrami equation

The kinetics of crystallization are generally interpreted with the Avrami equation,[22,23] which is essentially applicable to isothermal crystallization conditions. The nonisothermal aspect of crystallization is

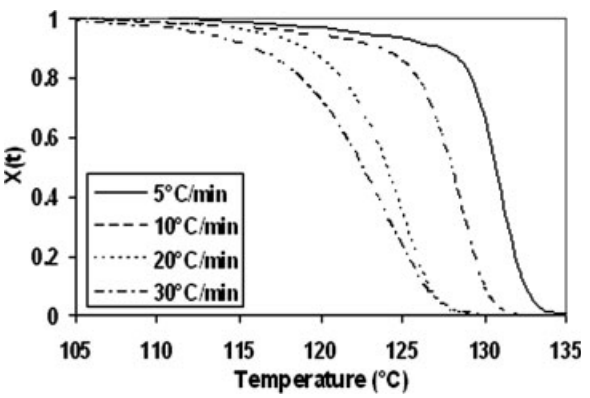

Figure 4 Curves of $X(t)$ versus the temperature for PP at various cooling rates calculated from the crystallization exotherm of PP.

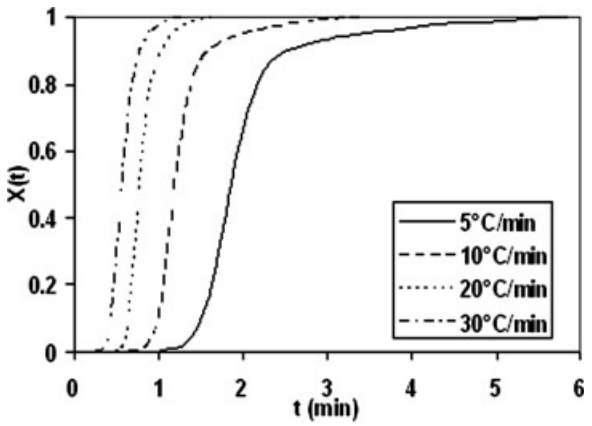

Figure 5 Curves of $X(t)$ versus time t for PP at various cooling rates calculated from crystallization exotherms.

inherent in the Avrami equation through time-dependent nucleation. According to the Avrami equation [eq. (2)], $X(t)$ at time t (i.e., the interval from $t = 0$ to $t = t$) is expressed as follows:

$$X(t) = 1 - \exp[-kt^n] \quad (2)$$

where k is a constant related to the crystallization rate and n is a parameter (known as the Avrami exponent) related to the nucleation type and growth geometry of the crystallization occurring. The double logarithmic form of eq. (2) leads to a linear plot between $\log\{-\ln[1 - X(t)]\}$ and $\log t$ yielding values of n and k through its slope and intercept.

Values of Avrami parameters n and k, obtained from the crystallization exotherms at various cooling rates, are shown in Table IV. The values were calculated for the $X(t)$ range of 10–80%. From Table IV, it can be seen that, although the values of n are noninteger, the values are very close to 4 at the cooling rate of 5°C/min, indicating spherulitic growth from sporadic nucleation. However, as the cooling rate increases, the n value decreases, and at the cooling rates of 20 and 30°C/min, the value of n is close to 3, indicating spherulitic growth from instantaneous nucleation. At the cooling rate of 10°C/min, the value of n is noninteger and lies between 3 and 4, indicating contributions from both sporadic and instantaneous nucleation. Moreover, the proportion of inclusions (i.e., nano-SiO_2 and PDMS) does not have a significant effect on the value of n.

Rate constant k increases with increasing cooling rate and this indicates a faster crystallization rate at a higher cooling rate. The values of k for PP/PDMS blends are higher than that of PP at all the cooling rates studied, and this indicates faster crystallization of PP in the presence of PDMS. However, there is no clear variation of k values observed with the PDMS content of the blend at any given cooling rate. The values of k for PP/nano-SiO_2 composites are lower than that of PP at lower cooling rates, and this indicates a slower crystallization rate of PP in the presence of nano-SiO_2 at lower cooling rates. However, at a high cooling rate (i.e., at 30°C/min), the values of k are higher than that of PP, and this indicates faster crystallization at this high cooling rate. These results are discussed in a later section.

On the basis of Tobin's equation

Furthermore, Tobin[24] proposed a different relationship by taking into account the growth site impingement and secondary crystallization effects. Tobin's equation expresses $X(t)$ as follows:

$$X(t) = \left[\frac{k_T t^{n_T}}{1 + k_T t^{n_T}}\right] \quad (3)$$

The subscript T is used to distinguish terms k and n of Tobin's equation from the corresponding terms in Avrami's equation. Values of k_T and n_T are determined from a linear plot of $\log\{X(t)/[1 - X(t)]\}$ versus $\log t$.

Values of Tobin parameters n_T and k_T, obtained from the crystallization exotherms at various cooling rates, are shown in Table V. The values were calculated for the $X(t)$ range of 10–80%. Similar variations can be observed in the values of n and k of Avrami analysis (Table IV) and n_T and k_T of Tobin analysis (Table V) with the cooling rates for all the samples. However, the values of Tobin's parameters (i.e., n_T and k_T) are higher

TABLE IV
Parameters of the Crystallization Kinetics from the Avrami Equation

Sample	Avrami exponent (n) at various cooling rates				Avrami rate constant (k) at various cooling rates			
	5 (°C/min)	10 (°C/min)	20 (°C/min)	30 (°C/min)	5 (°C/min)	10 (°C/min)	20 (°C/min)	30 (°C/min)
PP	4.29	3.97	3.36	3.36	0.49	4.68	16.98	25.12
PP/E5	3.83	3.48	2.96	2.90	0.95	3.80	16.98	32.36
PP/E10	3.97	3.64	3.14	3.18	0.79	5.25	16.60	40.74
PP/E20	4.00	3.57	3.16	2.98	0.81	5.89	20.89	41.69
PP/E30	3.98	3.67	3.13	3.09	0.91	5.75	19.05	38.02
PP/S2	4.20	3.72	3.19	3.05	0.42	3.16	13.80	24.55
PP/S4	4.49	3.66	3.10	3.16	0.26	2.69	12.30	30.90
PP/S6	3.98	3.37	3.25	2.98	0.39	2.88	14.45	28.18

TABLE V
Parameters of the Crystallization Kinetics from the Tobin Equation

Sample	Tobin exponent (n_T) at various cooling rates				Tobin rate constant (k_T) at various cooling rates			
	5 (°C/min)	10 (°C/min)	20 (°C/min)	30 (°C/min)	5 (°C/min)	10 (°C/min)	20 (°C/min)	30 (°C/min)
PP	5.43	5.25	4.29	4.44	0.72	14.45	42.66	128.82
PP/E5	4.97	4.64	3.94	3.92	1.78	10.96	77.62	204.17
PP/E10	5.28	4.64	4.27	4.15	1.35	14.79	83.18	229.09
PP/E20	5.36	4.70	4.20	3.90	1.38	19.05	107.15	251.19
PP/E30	5.48	4.75	4.09	4.07	1.66	17.38	87.10	218.78
PP/S2	5.47	4.81	4.04	4.08	0.62	8.13	52.48	125.89
PP/S4	5.95	4.79	3.94	4.10	0.32	6.76	43.65	158.49
PP/S6	5.06	4.44	4.13	3.90	0.55	7.41	53.70	144.54

than those of the Avrami parameters (i.e., n and k) for all the samples at all cooling rates.

Rate constant k_T increases with increasing cooling rate and this indicates a faster crystallization rate with the cooling rate increasing. The values of k_T for PP/PDMS blends are higher than that of PP at all the cooling rates studied, and this indicates faster crystallization in the case of PP/PDMS blend. However, there is no clear trend in the variation of k_T with the PDMS content of the blends at any given cooling rate. The values of k_T for PP/nano-SiO_2 composites are lower than that of PP, and this indicates a slower crystallization rate for PP in the presence of nano-SiO_2 at lower cooling rates (i.e., at 5 and 10°C/min). However, at the higher cooling rates (i.e., at 20 and 30°C/min), the k_T values are higher than that of PP. This cooling rate dependence on the crystallization rate is discussed below.

Effects of the cooling rate on crystallization

The effect of cooling rate on crystallization of PP in these composite and blend systems can be seen through a comparison of the $X(t)$–t plots at different

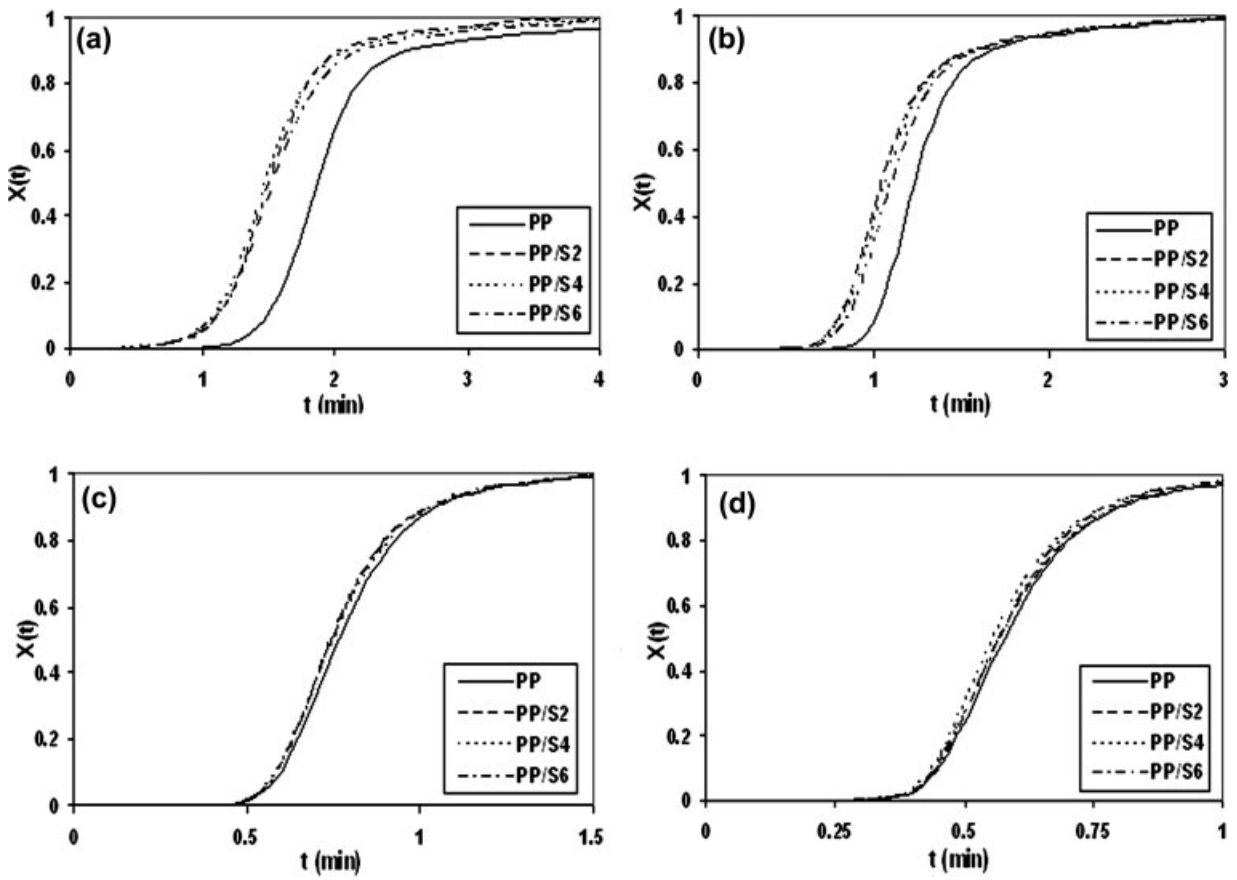

Figure 6 Plots of $X(t)$ versus time t for PP and PP/nano-SiO_2 composites at different cooling rates: (a) 5, (b) 10, (c) 20, and (d) 30°C/min.

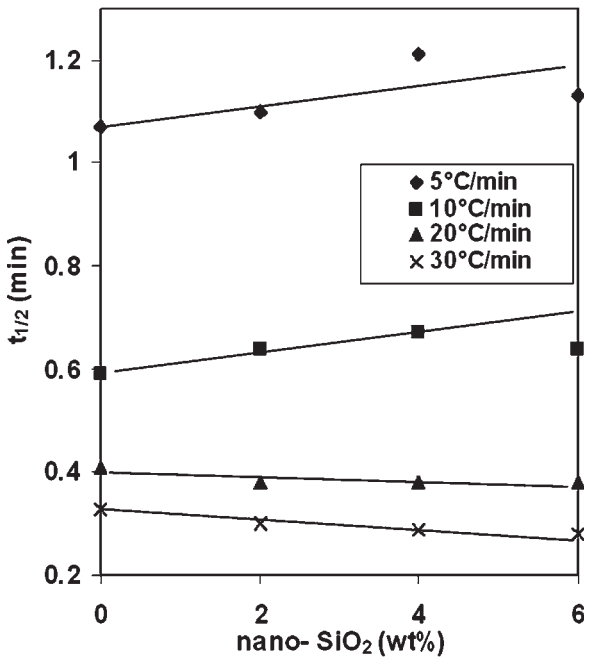

Figure 7 Plots of $t_{1/2}$ versus the nano-SiO_2 content at different cooling rates for PP/nano-SiO_2 composites.

cooling rates. These $X(t)$–t plots were derived from the corresponding crystallization exotherms with 140°C used as reference point 0 in the timescale. This representation gives an insight into the effect of the cooling rate on the overall crystallization process. The $X(t)$ vs t plots for PP/nano-SiO_2 system are shown in Figure 6. These $X(t)$–t curves indicate slow nucleation and rapid growth of crystallization in both systems. The slopes of the corresponding regions of the $X(t)$–t curves are compared to obtain information about the rates of the processes of nucleation and growth in the different systems.

PP/nano-SiO_2 composite

The $X(t)$–t curves of the PP/nano-SiO_2 composite system (Fig. 6) show that the entire process from nucleation to above 98% conversion takes more than 4 min at the cooling rate of 5°C/min and less than 1 min at the cooling rate of 30°C/min. There is gradual shift of the $X(t)$–t curve of the nanocomposite (dotted curves) toward that of PP (solid curve) with the cooling rate increasing [Fig. 6(a–d)]. This shows

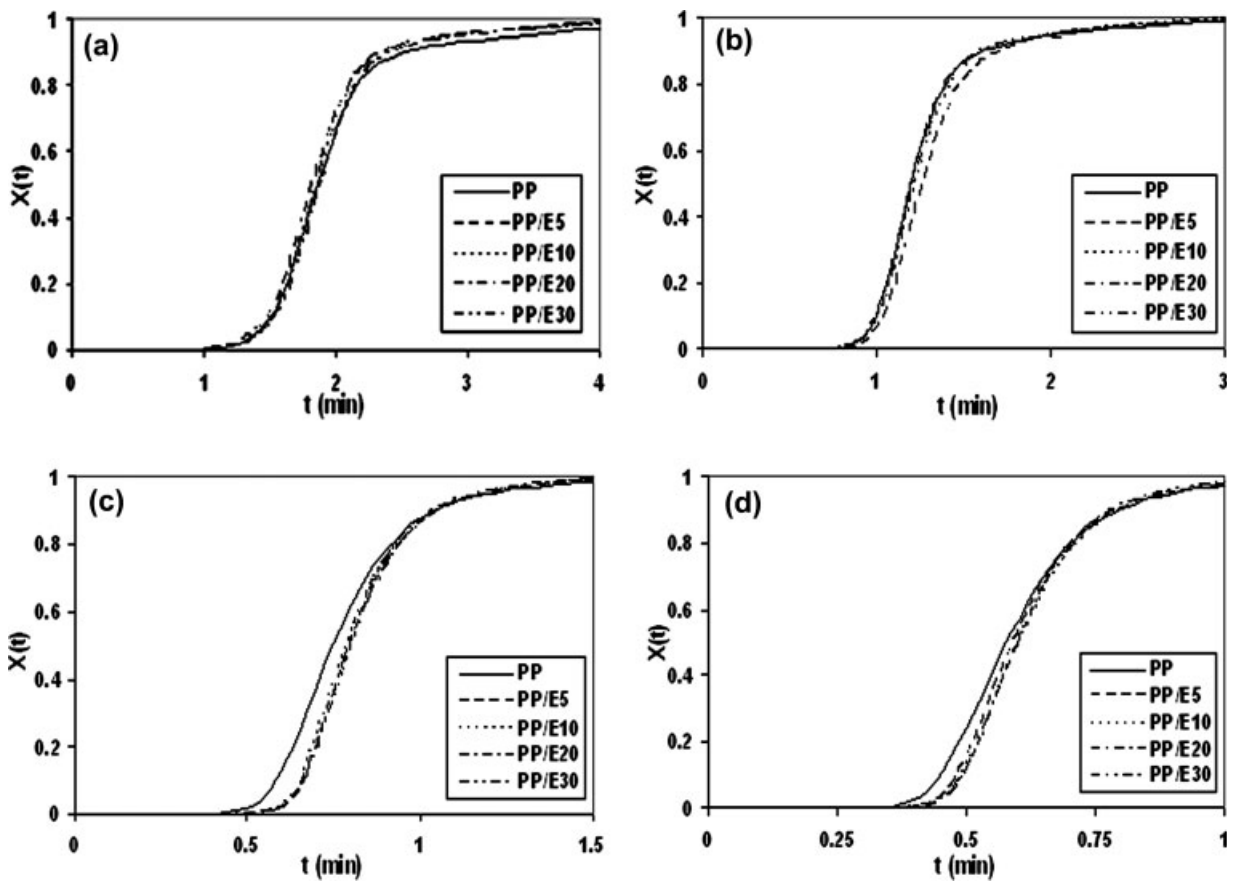

Figure 8 Plots of $X(t)$ versus time t for PP and PP/PDMS blends at different cooling rates: (a) 5, (b) 10, (c) 20, and (d) 30°C/min.

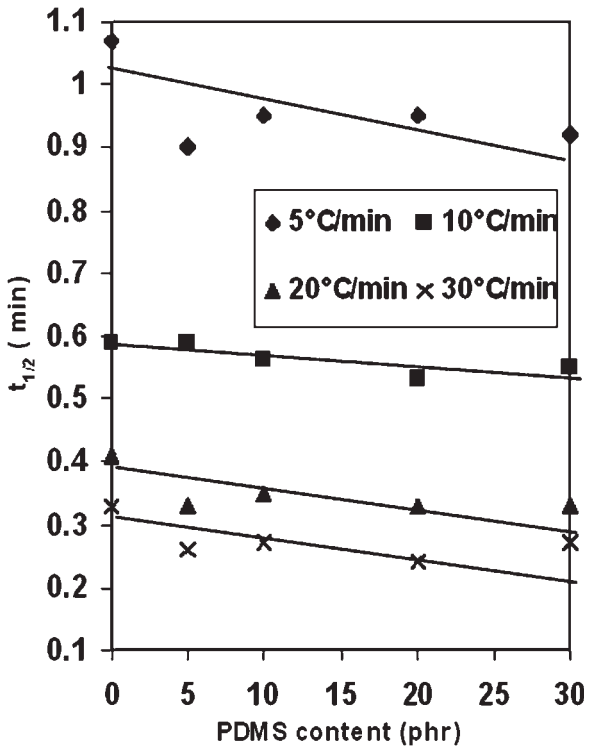

Figure 9 Variation of $t_{1/2}$ with the PDMS content at different cooling rates for the PP/PDMS blend system.

that the effect of nano-SiO_2 on the crystallization is more prominent only at low cooling rates rather than at high cooling rates. At low cooling rates, at which the nucleation occurs at relatively high temperatures, PP molecules get enough time for alignment to form stable nuclei, and this occurs preferentially on the nano-SiO_2 surface. On the other hand, at high cooling rates, the nucleation occurs instantaneously throughout the PP matrix. The variation of the half-time of crystallization ($t_{1/2}$) with the filler content (Fig. 7) shows higher values of $t_{1/2}$ at lower cooling rates (i.e., at 5 and 10°C/min) and lower values of $t_{1/2}$ at higher cooling rates (i.e., at 20 and 30°C/min), and this indicates slower and faster rates of crystallization at these lower and higher cooling rates, respectively. At higher cooling rates, the nucleation is apparently quite fast, and it may occur on the nano-SiO_2 surface, leading to an increase in the number of nucleation sites, which in turn results in a higher overall crystallization rate at higher cooling rates (i.e., at 20 and 30°C/min).

PP/PDMS blend

The $X(t)$–t curves for the PP/PDMS blend system (Fig. 8) show that the time required for the completion (i.e., from nucleation to 98% conversion) of the crystallization process is about 4 min at the cooling rate 5°C/min, and it gradually decreases as the cooling rate increases and is less than 1 min at the cooling rate 30°C/min. There is a shift of the initial portion of the $X(t)$–t curve away with respect to PP at the cooling rates of 20 and 30°C/min [Fig. 8(c,d)], indicating a delay in the nucleation process at higher cooling rates. However, after the nucleation, the slope of the growth region of the curve is higher than that of PP, indicating a faster crystallization rate for the PP/PDMS system. The $t_{1/2}$ values shown in Figure 9 are also in line with this observation, being lower for the blends than PP.

It seems that although PDMS slows down the nucleation process, the crystallization growth rate is higher, and this may be due to some ease of molecular segmental mobility caused by the presence of PDMS chains. This increased crystallization rate is very visible at the upper end of the crystallization curve (i.e., beyond 80% relative crystallinity), as shown in Figure 10(a) for the PP/PDMS blend at the cooling rate 5°C/min, in an extended scale. The chain mobility of PDMS at the interface of PP/PDMS blend domains may have facilitated the molecular mobility of PP during the crystallization process.

Activation energy

Various methods have been used[25–27] for the calculation of the activation energy of crystallization (ΔE);

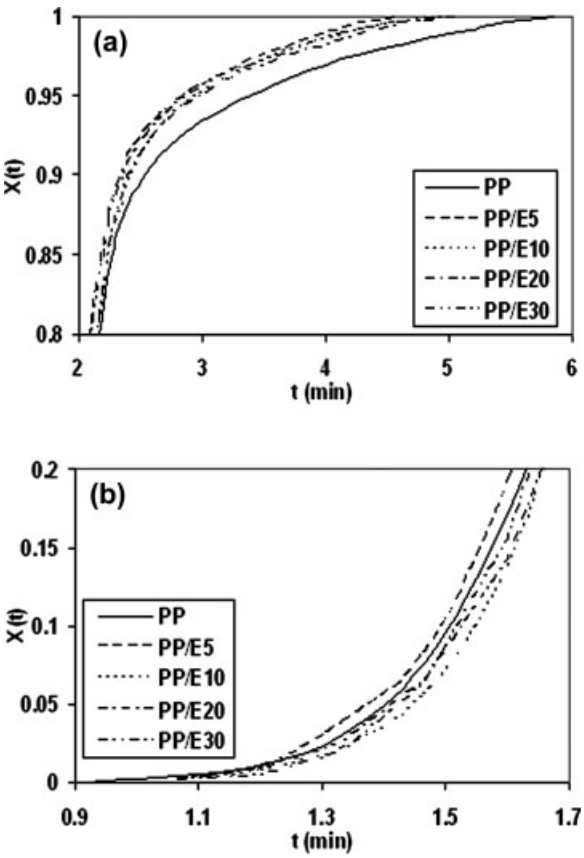

Figure 10 Plots of $X(t)$ versus time t for PP/PDMS blends at the cooling rate of 5°C/min: (a) above 80% relative crystallinity and (b) below 20% relative crystallinity.

TABLE VI
ΔE Values of PP, PP/PDMS Blends, and PP/Nano-SiO_2 Composites

Sample	ΔE (kJ/mol)
PP	338.23
PP/E5	324.51
PP/E10	325.90
PP/E20	312.95
PP/E30	311.15
PP/S2	288.70
PP/S4	287.32
PP/S6	285.70

we use here one of these methods, the Kissinger equation, without any reason for its preference:[25]

$$\left[\frac{d[\ln(P/T_p^2)]}{d(1/T_p)}\right] = -\frac{\Delta E}{R} \tag{4}$$

where T_p is the crystallization temperature at the peak maximum, R is the universal gas constant, and P is the cooling rate. The linear plot of the numerator versus the denominator of the left-hand side of eq. (4) gives a slope of $-\Delta E/R$, and the values of ΔE calculated from these slopes are given in Table VI.

The ΔE values for the PP/PDMS blend are lower than that of PP, showing a decreasing trend with increasing PDMS content. It may be noted that despite its delaying effect on nucleation, the PDMS elastomer produces a decrease of ΔE, and the decrease is proportional to the elastomer content. In the case of the PP/nano-SiO_2 composite, a more pronounced decrease of ΔE is observed with the initial 2 wt % filler addition, and thereafter very little decrease is shown with increasing filler content. This indicates the easing of crystallization process, which is apparently in contradiction to the trend of variation of ΔH_c. This inconsistency of the trends of variation of ΔE (Table VI) and ΔH_c (Table III) supports the contention of Matusita and Sakka[28] that Kissinger's method for activation energy is better suited to an n-order process than the nucleation and growth mechanism of crystallization.

CONCLUSIONS

The rate constants and the $t_{1/2}$ values showed faster crystallization of PP in the presence of PDMS at all the cooling rates studied. ΔE decreased upon the addition of the PDMS elastomer, and the decrease was proportional to the elastomer content. This can be attributed to the high chain mobility of PDMS molecules at the interface, which might facilitate molecular mobility of PP to enable it to orient and align in a crystalline lattice with ease. The reduced value of ΔE also supports this ease of crystallization.

The addition of nano-SiO_2 showed higher nucleating ability than PDMS in PP. The rate constants and the $t_{1/2}$ values showed slower crystallization of the PP/nano-SiO_2 composite compared to that of PP at cooling rates of 5 and 10°C/min but faster crystallization at 20 and 30°C/min. ΔE decreased significantly upon the addition of nano-SiO_2.

The values of n for both systems were close to 4 at lower cooling rates but gradually decreased to a value of 3 at higher cooling rates, indicating a change in the nature of nucleation from sporadic to instantaneous as the cooling rate increased. The values of n_T were higher than those of n. There was no significant variation observed in the values of these exponents upon the incorporation of nano-SiO_2 or PDMS elastomer.

References

1. Maiti, S. N.; Mahapatro, P. K. J Appl Polym Sci 1991, 42, 3101.
2. Menczel, J.; Varga, J. J Therm Anal 1983, 28, 161.
3. Busigin, C.; Lahtinen, R.; Thomas, G.; Woodhams, R. T. Polym Eng Sci 1984, 24, 169.
4. He, J. D.; Cheung, M. K.; Yang, M. S.; Qi, Z. J Appl Polym Sci 2003, 89, 3404.
5. Mucha, M.; Marszalek, J.; Fidrych, A. Polymer 2000, 41, 4137.
6. Lozano, K.; Barrera, E. V. J Appl Polym Sci 2001, 79, 125.
7. Bhattacharyya, A. R.; Sreekumar, T. V.; Liu, T.; Kumar, S.; Ericson, L. M.; Hauge, R. H.; Smalley, R. E. Polymer 2003, 44, 2373.
8. Arroyo, M.; Manchado, M. A. L.; Avalos, F. Polymer 1997, 38, 5587.
9. Quian, J.; He, P.; Nie, K. J Appl Polym Sci 2004, 91, 1013.
10. Fu, B. X.; Yang, L.; Somani, R. H.; Zong, S. X.; Hasio, B. S.; Phillips, S.; Blanski, R. J Polym Sci Part B: Polym Phys 2001, 39, 2727.
11. Martuscelli, E.; Silvestre, C.; Bianchi, L. Polymer 1983, 24, 1458.
12. Bartczak, Z.; Galeski, E.; Kasanikova, N. P. Polymer 1987, 28, 1627.
13. Zang, M.; Liu, Y.; Zhang, X.; Gao, J.; Huang, F.; Song, Z.; Wei, G.; Qiao, J. Polymer 2002, 43, 5133.
14. Li, C.; Tian, G.; Zhang, Y.; Zhang, Y. Polym Test 2002, 21, 919.
15. Gupta, A. K.; Gupta, V. B.; Peters, R. H.; Harland, W. G.; Berry, J. P. J Appl Polym Sci 1982, 27, 4669.
16. Quan, H.; Li, Z. M.; Yang, M. B.; Lu, Z. Y. J Macromol Sci Phys 2005, 44, 761.
17. Xu, G.; Shi, W.; Hu, P.; Mo, S. Eur Polym J 2005, 41, 1828.
18. Seo, Y.; Kim, J.; Kim, K. U.; Kim, Y. C. Polymer 2000, 41, 2639.
19. Bandrup, J.; Immergut, E. H. Polymer Handbook; Wiley: New York, 1975.
20. Di Lorenzo, M. L.; Silvestre, C. Prog Polym Sci 1999, 24, 917.
21. Marco, C.; Ellis, G.; Gomez, M. A.; Arribas, J. M. J Appl Polym Sci 2002, 84, 2440.
22. Avrami, M. J Chem Phys 1939, 7, 1103.
23. Avrami, M. J Chem Phys 1940, 8, 212.
24. (a) Tobin, M. C. J Polym Sci Polym Phys Ed 1974, 12, 399; (b) Tobin, M. C. J Polym Sci Polym Phys Ed 1976, 14, 2253; (c) Tobin, M. C. J Polym Sci Polym Phys Ed 1977, 15, 2269.
25. Kissinger, H. E. J Res Natl Bur Stand 1956, 57, 217.
26. Augis, J. A.; Bennett, J. E. J Therm Anal 1978, 13, 283.
27. Takhor, R. L. Advances in Nucleation and Crystallization of Glasses; American Ceramics Society: Columbus, OH, 1971; p 166.
28. Matusita, K.; Sakka, S. J Non-Cryst Solids 1980, 38, 741.